Discover Geoscience

Research

Assessment of gold mineralization potential in the Tanzania Craton based on stream sediment geochemistry multivariate analysis and regression modeling

Mahamuda Abu[1] · **John Desderius Kalimenze**[2,3] · **Benatus Norbert Mvile**[4] · **Samuel Nunoo**[5,6]

Received: 4 September 2024 / Accepted: 9 January 2025
Published online: 20 January 2025

Abstract
The artisanal and small-scale mining (ASSM) sector has contributed to economies and is an integral component of the drivers of the gross domestic product (GDP) of most developing countries. To enhance the production of the ASSM sector, most gold (Au) endowed countries have supported the sector's activities in diverse ways. However, despite this support, several factors, including poor exploration targeting, still affect the sector's production. This study, therefore, seeks to characterize the gold (Au) mineralization and its spatial distribution in the Singida region of the Tanzania Craton with a focus on identifying potential Au mineralized zones that could be demarcated and targeted for ASSM activities and further exploration exercises within the region. The study leverages stream sediment geochemical results to identify the elemental associations and pathfinder elements using multivariate statistics (Principal component analysis), multilinear regression modeling, and spatial distribution of Au and the pathfinder elements within the study area. The Au deposits in the area are strongly associated with the elements; Ni, Cr, V, Mg, Fe, Cu, and Al. Palladium (Pd), platinum (Pt), arsenic (As), and copper (Cu) are the main pathfinder elements in the area. Lead is not directly related to Au from the study. Mafic, ultramafic rocks, and clays are the most probable sources of Au in the area. Gold concentrations are focused on the southwestern fringes of the area. Southwestern, central south, and southeastern fringes of the area should also be explored considering the distribution of the dominant pathfinder elements. Alluvial and lateritic materials are also worth exploring.

Keywords Stream sediments · Geochemistry · Multivariate statistics · Regression modeling · Gold mineralization · Singida region—Tanzania

1 Introduction

Globally, the economies of developing countries especially, those endowed with natural resources such as Au, have benefited significantly from it [1, 2]. Gold has been one of the key drivers of the gross domestic product (GDP) within the African continent and other developing countries [3]. In the extracting sector of Au, artisanal and small-scale

✉ Benatus Norbert Mvile, benimvile98@gmail.com | [1]Department of Geological Engineering, School of Engineering, University for Development Studies, Nyankpala, P. O. Box 1882, Tamale, Ghana. [2]Geological Survey of Tanzania (GST), P. O. Box 903, Dodoma, Tanzania. [3]Department of Geography and Geology, University of Turku, 20014 Turku, Finland. [4]Department of Physics, College of Natural and Mathematical Sciences, University of Dodoma, P. O. Box 259, Dodoma, Tanzania. [5]Department of Earth Science, School of Physical and Mathematical Sciences, College of Basic and Applied Science, University of Ghana, P. O. Box LG 58, Legon, Ghana. [6]Department of Geology, University of Johannesburg, Auckland Park Kingsway Campus, Johannesburg, South Africa.

miners (ASSM) are key stakeholders and have been the backbone of many economies within Africa and other developing countries globally. Also, the ASSM sector and its activities have been a major source of employment and livelihood [4]. For the role that ASSM plays in many economies' growth, some governments including Tanzania recognize the ASSM sector contribution and have over the years made efforts towards creating an enabling environment that will enhance the sectors' growth, expansion, and contribution to Tanzania's economy [4]. For instance, the Tanzania government recognizing the ASSM contribution to the GDP growth of the country, has a vision to increase the sector's contribution to the GDP by 2025. Hence, to achieve this vision, the government of Tanzania demarcated areas within known mineralized regions in the country for ASSM activities. Albeit this commitment of the government to increase ASSM contribution to the GDP in the Tanzania Government Vision 2025, the production of the sector is still not significant and hence has been unable to meet its GDP contribution targets set by the government [4]. Several reasons including poor ore processing, poor mineralization targeting, lack of understanding of the type or style of mineralization, and lack of know-how in the control of mineralization among others, might have accounted for the low production by the ASSM companies.

Geochemistry over the years has proven to be a suitable and effective tool in exploration and in delineating mineralized zones, thus anomalous zones, in both brown and green fields [5–11]. The Singida region (Fig. 1) belongs to the broader Tanzania Craton (TC) and is endowed with numerous precious metals including Au due to the geological architecture therein [12]. The Singida region is currently the host to several Au mining companies in the Geita belt, Seza areas, Mbeya, and Geita—Kahama areas [13–18]. Although the Singida gold province, is well endowed with Au, one of the likely reasons for the low Au productivity by the ASSM is that their current locations were not sited through systematic geological evaluation and exploration techniques. There is a need for proper delineation of mineralized zones within the Singida Au province where these ASSM companies can be relocated to enhance their production as a Au extraction sector as well as a stakeholder of the economic drivers of the country.

Multivariate statistical approaches like hierarchical cluster analysis (HCA), principal component analysis (PCA), and factor analysis (FA), have been effective in constraining pathfinder elements and the contribution of the geology in the mineralization [9, 10, 19]. Trace elements in particular together with multivariate statistics have been extensively used as a preliminary exploration approach in targeting mineralized zones within a prospect for further exploration exercises [10, 11, 20, 21]. Recent studies have also shown that machine learning techniques multilinear regression modeling (MLR), random forest (RF), artificial neural network (ANN), etc. have proven robust in the characterization and forecasting of geological processes [54]. These methods have been applied extensively in geo-resource characterization such as groundwater and mineral prospecting, and have been combined with and without multivariate statistics by some researchers [22–27]. For instance, some recent advances have demonstrated the effectiveness of combining geostatistical algorithms of hybrid optimizations and K-Clustering in other metals of Cu exploration or detection [52, 53]. Hence, this study was conducted to characterize the Au mineralization in the Singida region with the main aim of delineating Au-rich areas that could be targeted for ASSM activities, and also for further exploration purposes. This has been carried out using stream sediment geochemical data, multivariate statistical techniques, and multilinear regression modeling.

2 Geological setting

The Singida area (Fig. 1) is within the central parts of Tanzania with a total area of about 2,900 km^2. The area is part of the Tanzania Craton (TC) as described by Mvile et al. [10] and Kabete et al. [12]. The Singida area belongs to the central Dodoma geological province [28] with characteristic metamorphic rocks of both migmatite and gneiss facies [12]. The Dodoma geological system also has narrow greenstone belts with greenschist and amphibolite metamorphic facies. Granitoids are part of the principal lithologies within the area and are the main intrusive rocks in the area [12]. The metamorphic facies, the granitoids, and the greenstone belt rock suite (volcaniclastics, basalts, andesites, phyllites, etc.), define the Precambrian (Fig. 1) geological terrains in the area [29]. The geology of the area is similar to adjacent Mozambique, Usagaran, Ubendian, and Ruwenzori belts that border the TC to the northwest and south [14, 30]. Unlike the surrounding belts, the mineralization in the TC is reported to have been hydrothermally controlled [31] predominantly. Mvile et al. [10] also reported a possible disseminated sulfide deposit type in the Dodoma region which is a lithologically controlled kind of mineralization. The ore-controlling minerals in the TC to which the Singida region belongs are sericite, calcite, silica, chlorite, epidote, and some silicate minerals. These are the main ore-controlling

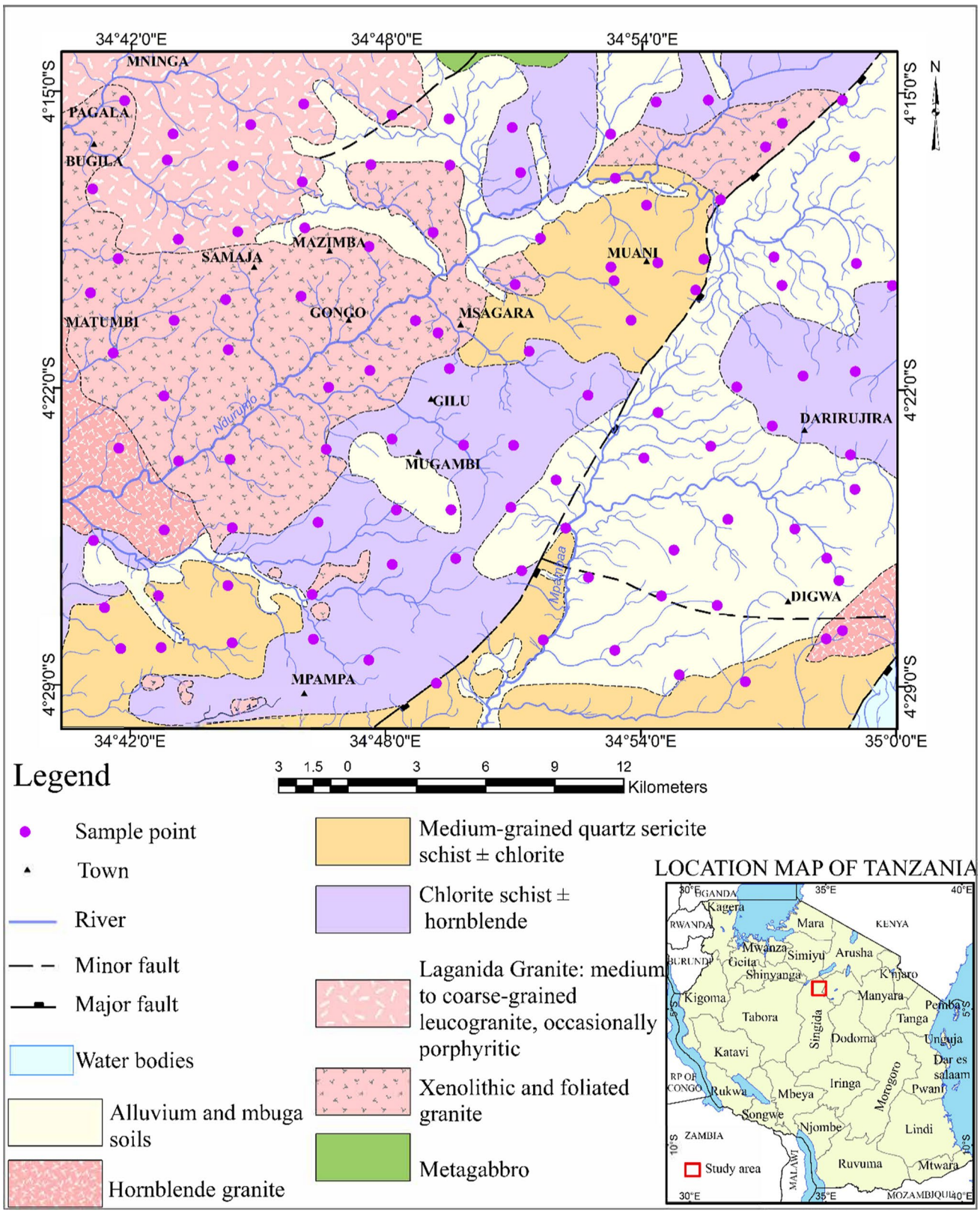

Fig. 1 The geological map of the Singida district of TC of Tanzania

minerals in greenstone belts globally [31]. The TC is deformed with evidence of faults and other brittle structures [32]. These brittle lineaments trend in NE, NW, and ESE directions in the region.

3 Materials and methods

3.1 Sampling and laboratory analysis

The stream sediment sampling methodology involved a systematic approach to ensure accurate and reliable results. Predefined sample points for stream sediment samples were identified, and the flood plains within the area were avoided during the sample selection. The samples were collected from first and second-order stream channels. A sample from three sub-homogenized samples was taken at each sampling site to represent the sample point. A total of 128 samples were collected, comprising 10 duplicate samples and 10 blank samples included for quality assurance (QA) and quality control (QC). These control samples were inserted successively after every 10 samples, and the blank samples mainly consisted of silica sand. The duplicates and blanks were used to verify the accuracy and reliability of the analytical procedure and laboratory results. The collected samples were air-dried and sieved in the field to the < 2 mm fraction. Subsequently, the samples were transported to the Geological Survey of Tanzania (GST) for further processing and analysis, where the samples underwent additional sieving to obtain the 75-micron fraction. Then after, the samples were transported to different laboratories for mineral or elemental analysis. The major oxide and trace element analysis was conducted at the Canadian Acme Laboratory (CAL) where the samples were prepared by undergoing a digestion process with an acid solution and were then analyzed using ICP-MS. The detection limits for the analysis were set between 0.0001% and 0.01% for oxides and 0.002 ppm and 2 ppm for trace elements. Additionally, the analysis of the gold–palladium-platinum group elements was performed at the Geological Laboratory of Henan in China where the samples underwent a series of preparation steps, including digestion with an acid solution, ashed, and dissolution. The resulting solution was analyzed using ICP-MS to determine the concentrations of Pt, Pd, and Au. The analytical procedures and protocols followed the analytical procedure of Mvile et al. [10].

3.2 Data exploration

Generally, geochemical data is not normally distributed, and hence for statistical approaches to be used in analyzing such data, it needs to be transformed to ensure it is normally distributed. Quantile–Quantile (Q-Q) plots have been used as a data exploration method [10] to observe the normality of geochemical data. In this study, the data exploration was done using Q-Q plots, and the raw and transformed data results are shown (Fig. 2a and b).

3.3 Data transformation

The data was not normally distributed in their raw form (Fig. 2a) and needed to be transformed to ensure a reduction in the outliers from Fig. 2b. The data were transformed using the centered log-ratio (clr) method and the details of the procedure can be found in Mvile et al. [10] and Sunkari et al. [33].

3.4 Statistical approaches

The correlation matrix is a primary statistical procedure that can bring out association patterns of compositional data e.g. geochemical data. This has been extensively applied to geochemical data to observe the elemental associations firsthand [10, 21]. Spearman's correlation was used as the first statistical approach in an attempt to identify the elemental and pathfinder associations within the area. Multivariate statistical methods were also applied as an advanced step to elucidate the elemental associations of the data set. Hierarchical cluster analysis (HCA) using the rescaled and average linkage methods and factor analysis (FA) with principal components (PCs) as the extracting methods, these methods have been suitable in this regard and have been extensively applied [10, 18, 34–37].

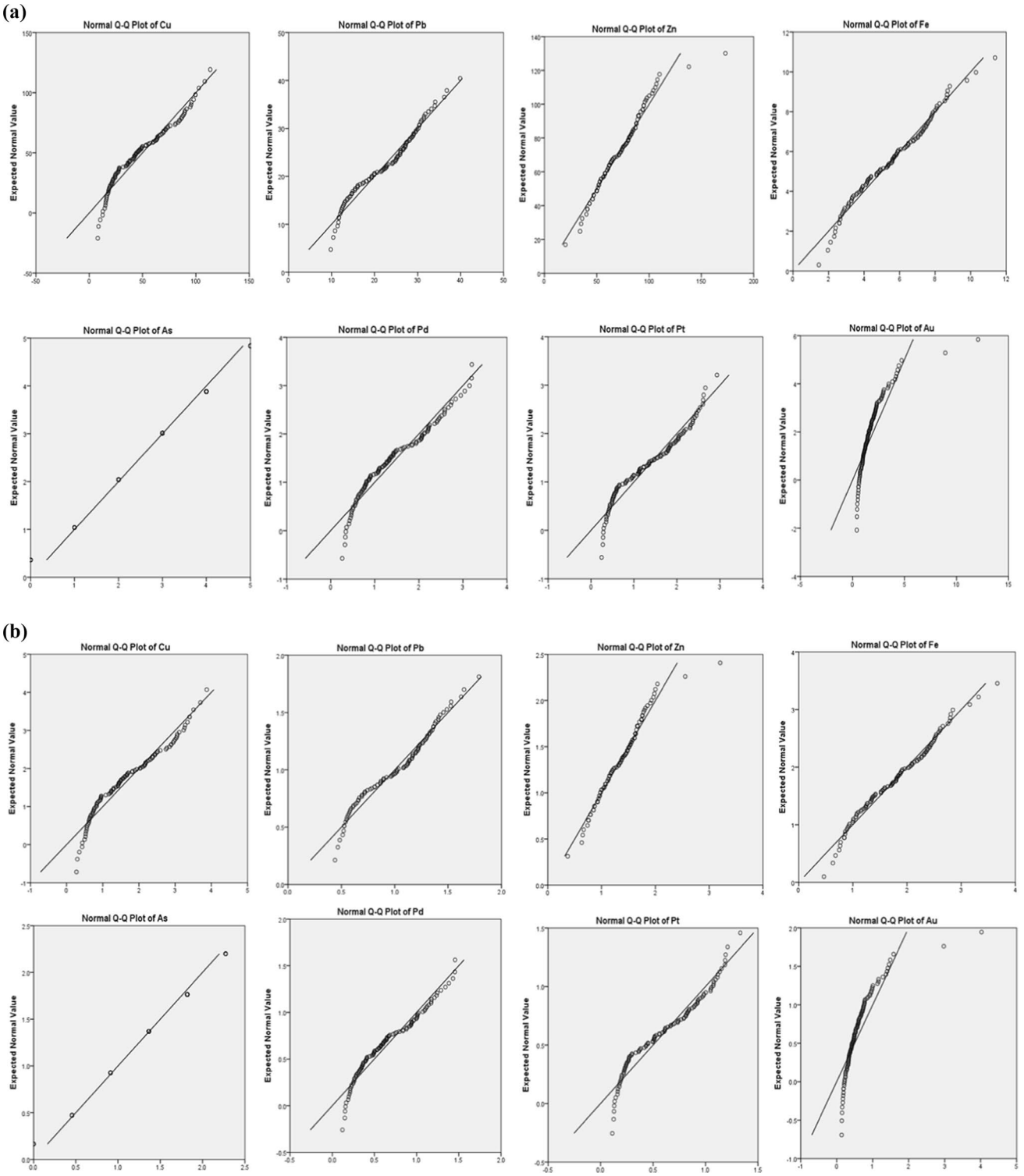

Fig. 2 **a** Q-Q plots of the untransformed data, Cu, Pb, Zn, Fe, As, Pd, Pt, and Au. **b** Q-Q plots of the clr transformed data for Cu, Pb, Zn, Fe, As, Pd, Pt, and Au

3.5 Multilinear regression

Multivariate linear regression (MLR) is a machine learning approach that is used in unraveling the association of several independent variables (trace elements and pathfinder elements) to a dependent variable (e.g. Au in this study) [38, 39]. A prediction model in the form of a mathematical equation indicates the level to which the independent variables contribute to the occurrence of the dependent variable. This has been effectively used to characterize groundwater [23, 24, 26, 27, 39]. The approach used to evaluate Au occurrence is still evolving. The prediction model for Au occurrence in the study area is as in Eq. 1.

$$y = b_0 + b_1 b_1 + b_2 b_2 + \ldots \ldots bixi + \varepsilon \quad (1)$$

where b_0 is the constant value in the model, x_i is the value of the ith predictor, the bi is the coefficient of the *i*th predictor, and for each individual *i* there is an error term ε.

3.6 Geochemical maps

In the generation of the plots and maps of the study, IBM SPSS version 20 and Surfer version have been used. The statistical analysis was done using IBM SPSS and Surfer was used in generating the interpolation maps for the spatial distributions.

4 Results and discussion

4.1 Trace element concentrations

The statistical summary of the untransformed trace elements concentration (Table 1) is widely varied, from 0.0 to 2937 ppm. The oxide concentration (in wt%) ranges between 0.0 and 12.1, with FeO having the highest concentration value of 12.1 wt%. The mean concentrations of the trace elements are as follows; Cu (26.65 ppm), Pb (22.63 ppm), Zn (58.07 ppm), Ni (31.98 ppm), Co (15.47 ppm), Mn (878.23 ppm), As (1.54 ppm), U (4.07 ppm), Th (29.38 ppm), Sr (147.67 ppm), V (90.66 ppm), La (65.30 ppm), Cr (71.78 ppm), and Ba (566.01 ppm). The precious group of elements (PGEs) is measured in ppb, with the following mean concentrations; Pd (0.78 ppb), Pt (0.79 ppb), and Au (1.35 ppb). The concentrations of the oxides are in the order of Fe > Al > K > Ti > Ca > Na > Mg. The concentrations of the trace elements are in the order of; Mn > Ba > Sr > V > Cr > La > Zn > Ni > Th > Pb > Cu > Co > U > As. The PGE content is in the order of Pd > Pt (Table 1). The order of the oxides suggests the dominance of the mafic rocks in the area over felsic rocks. Fe, Mg, Ti and Ca (in high temperature minerals), are high in mafic—ultra mafic minerals e.g. pyroxenes, hornblende and biotite. K, Ca, and Na are usually elements that are associated with the weathering of felsic minerals e.g. microcline, anorthite, and albite [10, 40–42]. The concentration of the oxides could be the result of the chemical weathering of both mafic and felsic rocks in the study area. Ni, Co, Cr, V, and Cu are known mafic minerals weathering products [43, 44], whereas Sr, Th, U, La, Rb, and Ba are often associated with the chemical weathering of felsic minerals [10, 41, 45]. The trace elements concentration corroborates with their oxides counterparts. According to Mshiu et al. [31], the primary lithology in the area consists of mafic and felsic rocks, along with their associated metamorphic suites. These lithologies are the dominant rock types present in the region. Also, Pb, Cu, Zn, As, Ag, and Sb are well-known pathfinder elements to Au occurrence [10, 21, 34], hence the presence of these elements is a strong indication of Au occurrence in these parts of the TC.

4.2 Multivariate statistics

4.2.1 Spearman's correlation

The elements of interest in the Spearman's correlation matrix presented in Table 2 are; Cu, Pb, Fe, As, Au, and Zn. Cu correlates positively and significantly with the following elements; Zn, Fe, Pd, Pt, Au, V, Cr, Mg, Ti, Sc, Ni, Co, and Mn. It also correlates with As positively but insignificant with r = 0.3 and correlates negatively with Pb (r = -0.3) (Table 2). Lead (Pb) also correlates positively with U, Th, La, K, and Rb and negatively with Au (r = -0.1), and Pt (r = -0.1) (Table 2). The following elements; Pd, Pt, Au, Cr, V, Ti, Al, Sc, and Au correlates positively although insignificant (r = 0.3), with

Table 1 Descriptive statistics of the untransformed and clr transformed data

	N	Minimum	Maximum	Mean	Std. Deviation	Variance
Cu	108.00	5.40	78.30	26.65	16.69	278.53
Pb	108.00	6.10	58.60	22.63	10.58	111.94
Zn	108.00	12.00	147.00	58.07	22.07	487.17
Ni	108.00	5.50	101.30	31.98	20.74	430.15
Co	108.00	2.50	53.60	15.47	9.98	99.53
Mn	108.00	153.00	2937.00	878.23	542.18	293,957.06
Fe	108.00	0.68	12.09	3.91	2.31	5.32
As	108.00	0.00	8.00	1.54	1.21	1.47
U	108.00	0.70	24.00	4.07	3.45	11.91
Pd	108.00	0.15	2.21	0.78	0.45	0.20
Pt	108.00	0.15	2.15	0.79	0.48	0.23
Au	108.00	0.36	9.13	1.35	1.35	1.81
Th	108.00	2.70	157.90	29.38	30.26	915.53
Sr	108.00	35.00	600.00	147.67	93.30	8705.46
V	108.00	15.00	299.00	90.66	59.02	3483.72
Ca	108.00	0.04	3.65	0.68	0.66	0.44
La	108.00	9.10	434.90	65.30	61.97	3840.85
Cr	108.00	14.00	190.00	71.78	37.70	1421.58
Mg	108.00	0.04	1.31	0.35	0.25	0.06
Ba	108.00	170.00	1689.00	566.01	262.02	68,654.76
Ti	108.00	0.17	3.78	1.06	0.64	0.42
Al	108.00	2.23	10.41	6.62	1.57	2.47
Na	108.00	0.10	2.45	0.95	0.65	0.43
K	108.00	0.28	4.59	2.09	1.03	1.07
Sc	108.00	1.00	34.00	9.74	6.67	44.55

Clr transformed data

	N	Minimum	Maximum	Mean	Std. Deviation	Variance	Skewness
Cu	108.00	-0.70	0.50	− 0.09	0.28	0.08	− 0.20
Pb	108.00	− 0.60	0.30	− 0.12	0.21	0.05	− 0.33
Zn	108.00	− 0.70	0.40	− 0.03	0.18	0.03	− 0.82
Ni	108.00	− 0.80	0.50	− 0.10	0.31	0.10	− 0.26
Co	108.00	− 0.80	0.50	− 0.09	0.27	0.08	− 0.09
Mn	108.00	− 0.80	0.50	− 0.07	0.24	0.06	0.10
Fe	108.00	− 0.80	0.50	− 0.08	0.25	0.06	− 0.14
As	108.00	− 0.20	0.70	0.05	0.17	0.03	0.43
U	108.00	− 0.80	0.80	− 0.13	0.32	0.10	0.07
Pd	108.00	− 0.70	0.40	− 0.08	0.26	0.07	− 0.18
Pt	108.00	− 0.70	0.40	− 0.09	0.28	0.08	− 0.12
Au	108.00	− 0.60	0.80	− 0.13	0.28	0.08	1.07
Th	108.00	− 1.10	0.70	− 0.19	0.38	0.15	0.08
Sr	108.00	− 0.60	0.60	− 0.09	0.26	0.07	0.02
V	108.00	− 0.80	0.50	− 0.08	0.27	0.07	0.03
Ca	108.00	− 1.20	0.70	− 0.17	0.38	0.14	0.02
La	108.00	− 0.90	0.80	− 0.14	0.31	0.10	0.27
Cr	108.00	− 0.70	0.40	− 0.07	0.24	0.06	− 0.27
Mg	108.00	− 1.00	0.50	− 0.16	0.29	0.08	0.04
Ba	108.00	− 0.50	0.50	− 0.04	0.21	0.04	− 0.23
Ti	108.00	− 0.80	0.50	− 0.09	0.25	0.06	− 0.22
Al	108.00	− 0.50	0.20	− 0.01	0.12	0.01	− 1.13

Table 1 (continued)

Clr transformed data							
	N	Minimum	Maximum	Mean	Std. Deviation	Variance	Skewness
Na	108.00	− 1.00	0.40	− 0.15	0.36	0.13	− 0.48
K	108.00	− 0.90	0.30	− 0.07	0.28	0.08	− 0.88
Sc	108.00	− 1.00	0.50	− 0.10	0.29	0.09	− 0.27
Rb	108.00	− 1.00	0.50	− 0.10	0.29	0.08	− 0.35

Fe (Table 2). Arsenic (As) also, has a positive correlation with Pd, Pt, Au, V, and Cr although insignificant with r = 0.3 (Table 2). Au correlates significantly (r = ≥ 0.5) with Ni, Pd, and Pt, it however correlates insignificantly with Cr (r = 0.3), Sc (r = 0.3), and Co (r = 0.4) (Table 2). Zinc (Zn) also correlates positively with Ni, Co, Mn, Fe, Pd, Pt, and Au (r = 0.3) (Table 2). The elements that correlate positively with Au (Table 2) are; Cu, Fe, As, Zn, Pd, and Pt. The significance (r = 0.5) of the correlation of the probable pathfinder elements to Au occurrence in the area is in the order of Pt > Pd > Cu > Fe, Zn > As. It can be concluded from the correlation matrix that, the elements that are associated with Au are; Cu, Fe, As, Zn, Pd, Pt, and Au, and in increasing correlation strength order of As < Zn, Fe < Cu < Pd < Pt < Au. The elemental association can be said to have been controlled by the mafic–ultramafic rocks in the area [10, 43] hence, the Au in the area could be said to be associated with mafic–ultramafic rocks in the area [10].

4.2.2 Cluster analysis

Hierarchical cluster analysis (HCA) is a powerful geochemical data analytical approach suitable for grouping the geochemical parameters and defining the elemental associations [10, 21, 27, 34]. The results of the HCA are presented in the form of a dendrogram (based on a normalized data set) using the average linkage (between groups) and rescaled distance method (Fig. 3). From the HCA (Fig. 3), three broad clusters have been identified with cluster 1 (C1) consisting of; Au, Pd, Pt, As, Al, Zn, Ti, Mn, Ni, Cu, Sc, V, and Fe. Cluster 2 (C2) has Mg, Ca, Na, and Sr defining that cluster, and cluster 3 (C3) contains Th, La, U, K, Rb, Pb, and Ba as its components. The elements; Au, As, Cu, Mn, Zn, Pb, and Fe are largely agreed as pathfinder elements to the occurrence of Au [10, 21, 34, 43]. Hence, the elemental association with these aforementioned pathfinder elements is the focus of the discussion. From the elemental association in C1, it is unequivocal, that the Au occurrence in the study area is associated with As, Zn, Mn, Cu, and Fe (Fig. 3). The presence of Al in sediments is mostly due to the contribution or presence of clay minerals [45, 46]. The association of Au with Al in C 1 (Fig. 3) is suggestive of the presence of alluvial Au deposits in the study. The following trace elements; Ti, Mn, Cu, V, Fe, Sc, and Zn, are common elements of high-temperature minerals of mafic–ultramafic rocks [41]. This means, therefore, that the Au occurrence in the area is associated with mafic–ultramafic rocks in the area. The relatively strong correlation of Au with the PGEs (Pd and Pt) in Table 2 has been unequivocally brought out again by the cluster analysis, with Au, Pd, and Pt defining an intracluster in C1 (Fig. 3). The Au in the area and these two PGEs are strongly related and areas with Au enrichments could be explored also for these two PGEs. Gold (Au) in ferruginous or lateritic materials is worth exploring with Au correlation with Fe (Table 2) and also in the same cluster (C1) with Fe (Fig. 3). The C2 (Fig. 3) could be explained by the effect of chemical weathering of felsic rocks in the area with the presence of Na, Ca, and Sr. These are common elements of silicate minerals like albite, anorthite, and plagioclase [47]. The presence of carbonate minerals with Mg and Ca, cannot also be precluded and might be present in the area. Cluster 2 most likely indicates the presence of felsic and carbonate rocks in the area, these rock suites, however, do not control the Au occurrence in the area from the HCA (Fig. 3). In C3, the elemental association of Th, La, U, K, Rb, and Ba is typical of felsic rocks [41, 46]. The association of Pb with these (Table 2) elemental suites suggests it is related to felsic rocks in the area. This pathfinder element, Pb, does not correlate with Au (Table 2) nor associate with Au (Fig. 3). Its association and correlation with these elements reaffirm the assertion that the Au in the area is not associated with the felsic rocks in the area under consideration. In all, the HCA indications corroborate with the correlation matrix and explicitly brought out the controls of the Au occurrences in the study area.

Table 2 Spearman's correlation matrix of the transformed data: Fe, Mg, Ca, Al, Na, and K (in wt %), Pd, Pt, and Au (in ppb) the trace elements (ppm)

	Cu	Pb	Zn	Ni	Co	Mn	Fe	As	U	Pd	Pt	Au	Th	Sr	V	Ca	La	Cr	Mg	Ba	Ti	Al	Na	K	Sc	Rb
Cu	1.0	0.5																								
Pb	− 0.3	1.0																								
Zn	0.7	0.0	1.0																							
Ni	0.9	0.2	0.7	1.0																						
Co	0.9	0.2	0.7	0.9	1.0																					
Mn	0.6	0.1	0.6	0.5	0.7	1.0																				
Fe	0.8	0.1	0.8	0.8	0.9	0.8	1.0																			
As	0.3	0.2	0.2	0.3	0.3	0.1	0.2	1.0																		
U	− 0.3	0.5	0.1	− 0.3	− 0.3	− 0.1	− 0.2	− 0.2	1.0																	
Pd	0.7	0.1	0.5	0.8	0.6	0.2	0.5	0.3	− 0.1	1.0																
Pt	0.7	− 0.1	0.6	0.8	0.7	0.3	0.6	0.2	− 0.1	0.8	1.0															
Au	0.5	− 0.1	0.3	0.5	0.4	0.0	0.3	0.3	− 0.2	0.6	0.6	1.0														
Th	− 0.3	0.6	0.0	− 0.3	− 0.3	0.0	− 0.1	− 0.1	0.9	− 0.1	− 0.2	− 0.3	1.0													
Sr	− 0.3	0.1	0.0	− 0.1	− 0.1	− 0.1	− 0.2	− 0.2	0.1	− 0.3	− 0.2	− 0.3	0.0	1.0												
V	0.8	0.1	0.7	0.8	0.9	0.8	0.9	0.3	− 0.3	0.4	0.5	0.2	− 0.2	− 0.1	1.0											
Ca	0.1	− 0.1	0.3	0.2	0.3	0.3	0.2	− 0.1	− 0.3	− 0.2	− 0.1	− 0.1	− 0.4	0.7	0.3	1.0										
La	− 0.1	0.7	0.2	− 0.2	− 0.1	0.1	0.0	− 0.1	0.8	0.0	− 0.1	− 0.2	0.9	0.0	− 0.1	− 0.3	1.0									
Cr	0.9	0.4	0.6	0.9	0.8	0.5	0.8	0.3	− 0.2	0.8	0.7	0.5	− 0.2	− 0.3	0.7	0.0	− 0.1	1.0								
Mg	0.6	0.1	0.6	0.7	0.7	0.4	0.5	0.1	− 0.3	0.4	0.4	0.2	− 0.4	0.4	0.6	0.7	− 0.2	0.5	1.0							
Ba	− 0.6	0.1	− 0.3	− 0.6	− 0.6	− 0.4	− 0.5	− 0.1	0.6	− 0.4	− 0.4	− 0.3	0.5	0.6	− 0.5	0.0	0.5	− 0.6	− 0.3	1.0						
Ti	0.6	− 0.1	0.6	0.4	0.6	0.9	0.8	0.1	0.0	0.2	0.2	0.1	0.1	− 0.3	0.8	0.1	0.2	0.4	0.2	− 0.3	1.0					
Al	0.4	0.4	0.5	0.4	0.3	0.2	0.5	0.1	0.4	0.2	0.2	− 0.1	0.4	0.0	0.4	0.0	0.4	0.3	0.2	0.0	0.3	1.0				
Na	− 0.4	− 0.4	− 0.1	− 0.3	− 0.3	− 0.3	− 0.4	− 0.3	0.0	− 0.4	− 0.4	− 0.3	− 0.1	0.8	− 0.3	0.6	− 0.2	− 0.5	0.2	0.4	− 0.4	− 0.1	1.0			
K	− 0.7	0.5	− 0.4	− 0.7	− 0.7	− 0.5	− 0.6	− 0.1	0.7	− 0.4	− 0.4	− 0.4	0.7	0.2	− 0.6	− 0.4	0.5	− 0.6	− 0.6	0.8	− 0.4	0.0	0.1	1.0		
Sc	0.9	0.0	0.8	0.9	0.9	0.7	0.9	0.2	− 0.2	0.6	0.6	0.3	− 0.2	− 0.2	0.9	0.3	− 0.1	0.8	0.6	− 0.6	0.6	0.5	− 0.3	− 0.7	1.0	
Rb	− 0.5	0.7	− 0.3	− 0.5	− 0.6	− 0.4	− 0.5	− 0.1	0.7	− 0.2	− 0.3	− 0.3	0.7	− 0.1	− 0.5	− 0.6	0.6	− 0.4	− 0.6	0.6	− 0.3	0.2	− 0.1	0.9	− 0.5	1

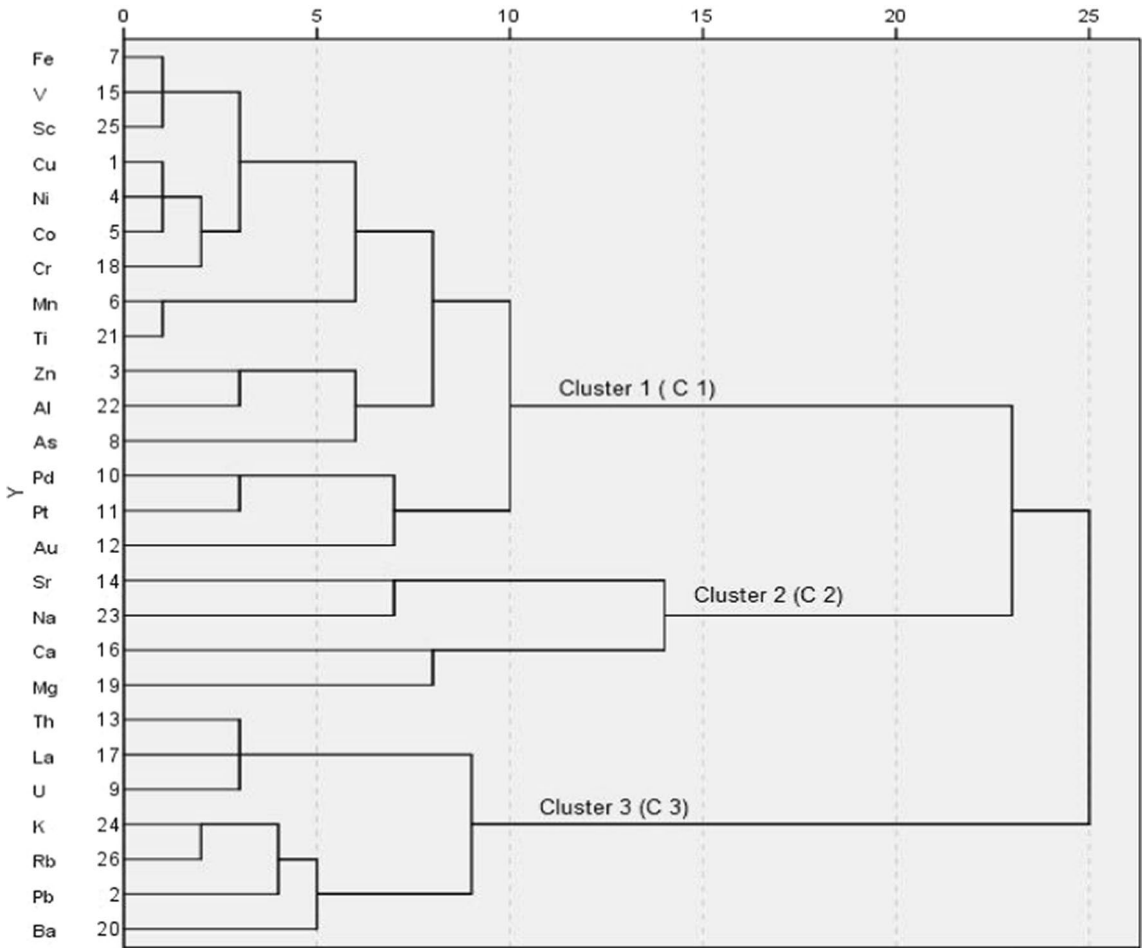

Fig. 3 Dendrogram of the hierarchical cluster analysis of the clr transformed data

4.2.3 Factor analysis

Principal component analysis (PCA) is one of the most used multivariate statistical approaches in elucidating geochemical and hydrochemical parameters [10, 11, 33, 34, 48]. The PCA method was applied to the normalized data set and the extraction method applied in the factor analysis (FA) was the principal component (Table 3). The relevance and deduction of the number of components or principal components (PC), depends on the eigenvalues during the analysis, and eigenvalues > 1 are often loaded and considered to have played a role in the evolution of the geochemical data under consideration. The scree plot (Fig. 4a) is also one of the plots that help to provide a ready visual grouping of the principal components. In that also, the number of the eigenvalues > 1 defines the expected number of PCs, and this indicates a point on the plot where the line begins to level out and becomes horizontal with the abscissa (points above the thin red horizontal line in Fig. 4a). The FA of the data loaded 4 PC (Table 3 and Fig. 4b) with PC1 accounting for 44.36% of the total variance, PC2, PC3, and PC4 also accounted for 18.60, 12.18, and 7.33%, respectively. These four PCs accounted for 82.47% of the total variance (Table 3). In Table 3, PC1 has Cu, Zn, Ni, Co, Mn, As, Pt, Pd, Au, V, Cr, Mg, and Ti defining that component. Pb, U, Th, Al, K, Rb, and La also define PC2. PC3 also contains Sr, Ca, Ba, and Na while PC4 has significant loading although < 0.5, are Pd, Pt, and Au (Table 3). PC1 elemental association is typical of high-temperature minerals and mafic–ultramafic rocks association with Au, this corroborates with cluster analysis and the interpretation thereof. PC2 and PC3 are the results of felsic minerals bearing rocks weathering in the area and corroborate the interpretation that, Pb is associated with the felsic rocks in the area and might not be a pathfinder of Au in the study area. PC4 appears to be reaffirming the strong association of Au to the Pd and Pt, and vice versa.

The plot of the rotated loadings in space (Fig. 4) of the factor analysis (FA) has been grouped also, into 4 factors (F), with F1, having the following elemental association; Cu, Sc, Cr, Ni, Co, Mg, V, Fe, Ti, Mn, and Zn (Fig. 4). Factor 2 (F2), has Na, Sr, Al, and Ca with Pb, U, Th, La, Ba, K, and Rb in F3 and F4 containing Pd, Pt, Au, and As (Fig. 4). The plot of the factor

Table 3 Extracted principal components eigenvalues loadings and principal components using the clr transformed data

	Initial Eigenvalues			Extraction sums of Squared Loadings			Rotation sums of Squared Loadings		
	Total	% of Variance	Cumulative %	Total	% of Variance	Cumulative %	Total	% of Variance	Cumulative %
1	11.53	44.36	44.36	11.53	44.36	44.36	7.53	28.95	28.95
2	4.84	18.60	62.96	4.84	18.60	62.96	5.70	21.94	50.88
3	3.17	12.18	75.14	3.17	12.18	75.14	5.18	19.93	70.81
4	1.91	7.33	82.47	1.91	7.33	82.48	3.03	11.66	82.47

Principal components				
	1	2	3	4
Cu	**0.93**	0.20	− 0.05	0.08
Pb	− 0.53	**0.76**	0.06	0.21
Zn	**0.73**	0.35	0.37	0.08
Ni	**0.93**	0.13	0.01	0.26
Co	**0.94**	0.12	0.12	0.01
Mn	**0.68**	0.20	0.31	− 0.52
Fe	**0.90**	0.27	0.15	− 0.20
As	**0.29**	0.11	− 0.28	0.16
U	− 0.45	**0.77**	0.29	0.11
Pd	**0.64**	0.34	− 0.33	**0.48**
Pt	**0.70**	0.24	− 0.23	**0.44**
Au	**0.46**	0.05	− 0.45	**0.44**
Th	− 0.45	**0.82**	0.22	− 0.07
Sr	− 0.22	− 0.29	**0.78**	0.39
V	**0.89**	0.17	0.22	− 0.22
Ca	0.28	− 0.52	**0.75**	0.10
La	− 0.28	**0.83**	0.26	− 0.02
Cr	**0.85**	0.23	− 0.18	0.19
Mg	**0.69**	− 0.23	0.49	0.33
Ba	− 0.71	0.24	**0.38**	0.21
Ti	**0.61**	0.33	0.18	− 0.56
Al	0.28	**0.57**	0.38	0.07
Na	− 0.35	− 0.49	**0.64**	0.29
K	− 0.83	**0.42**	0.05	0.11
Sc	**0.91**	0.20	0.16	− 0.04
Rb	− 0.68	**0.61**	− 0.11	0.05

loadings is similar to the PC and the same interpretations can be made for the factor plots as it is in the case of the PC. It is, however, worth noting that, As appears to be associated with Pd, Pt, and Au (Fig. 4), and as such, could be said to be the most probable pathfinder element to all the three minerals, thus Au, Pd, and Pt.

4.2.4 Pathfinder elements

The elemental association shows that Au has a good relation with Zn, Fe, As, Cu, Pd, and Pt. These associations can be seen in the correlation matrix (Table 1), the CA (Fig. 3), PCA (Table 3), and FA (Fig. 4). Au is in C1 together with Al (Fig. 3) suggesting its positive relation with Al. When sulfides and phyllosilicate minerals are exposed to the surface, they undergo oxidation to form Fe–oxides and clay minerals [10, 49]. However, as one of the known and common pathfinder elements in Green Stone Belts [21, 34, 50], Pb is not seen to be associated with Au from all the aforementioned analytical approaches during the study, hence not a pathfinder element in the study area. From the study, the elements that can be used as tracers for the occurrences of Au in the area are; Zn, Cu, As, Pd, Pt, Fe, and Al. The prominence of these pathfinder elements from the study is in the order of Pt > Pd > Cu > Fe > Zn > As > Al.

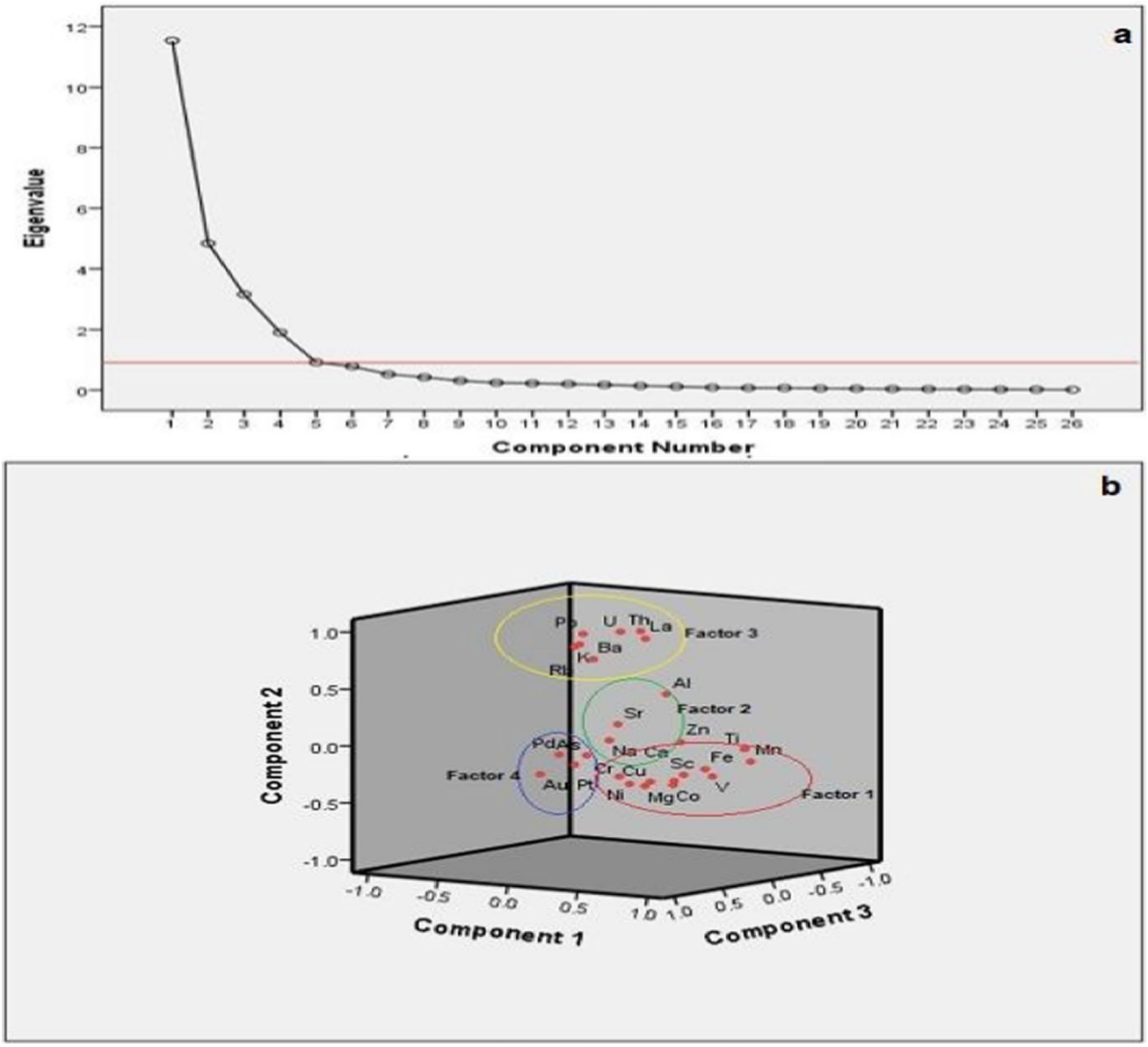

Fig. 4 Scree plot of eigenvalues versus components, a, rotated component loadings plotted in space, b

4.3 Prediction model for Au

The multivariate linear regression (MLR) model has been used in deciphering the number of predictors of a parameter when applied to compositional data [51]. In that, the relationship of a number of predicting variables/parameters (independent variables) together with a dependent variable/parameter, is well constrained [38].

In the MLR, Cu, Pb, Ni, Co, Mn, As, Pd, Pt, Fe, V, and Cr were used as the independent elements for Au occurrences in the area (Table 4). These are pathfinder elements and elements believed to be of mafic–ultramafic rock suite. Among the coefficients of the elements considered, the standardized coefficients of these elements indicate their usability as Au indicators in the area, and from Table 4, the standardized coefficient shows that Au can be predicted by Pd, Cu, Pt, Cu, Cr, As and V. These accounts for 52% (R square value) of the variance in Au occurrence, which is significant couple with a test of significance value (F–) of 9.553. They are in the order of Pd > Pt > Cu > V > Cr > As (Table 4). The prediction model for Au in the area is;

Table 4 Estimates of the elements as predictors of Au in the prediction model

Model	Unstandardized Coefficients		Standardized Coefficients	t	Sig
	B	Std. Error	Beta		
(Constant)	− 0.135	0.029		− 4.731	0.000
Cu	0.223	0.251	0.229	0.890	0.376
Pb	− 0.367	0.112	0.284	− 3.260	0.002
Ni	− 0.348	0.318	0.393	− 1.093	0.277
Co	− 0.083	0.327	0.082	− 0.254	0.800
Mn	− 0.071	0.188	0.063	− 0.381	0.704
As	0.141	0.130	0.084	1.087	0.280
Pd	0.547	0.181	0.511	3.023	0.003
Pt	0.339	0.153	0.338	2.220	0.029
Fe	− 0.220	0.248	0.196	− 0.885	0.378
V	0.163	0.213	0.107	0.768	0.444
Cr	0.113	0.227	0.098	0.499	0.619

$$Au = -0.135 + 0.511Pd + 0.338Pt + 0.229Cu + 0.107V + 0.098Cr + 0.084As + 0.029 \quad (2)$$

The prediction coefficients of the elements agree with the observation made in the factor analysis with the significance of the pathfinder elements being in the order of Pd > Pt > As > Cu from the T-values (Table 4). The other parameters in the model (Eq. 2); V, and Cr could be explained that the Au occurrence is much associated with the mafic–ultramafic rocks in the area.

4.4 Geostatistics

The spatial distribution of the pathfinder elements from the various assessment methods adopted in the study and Au is shown in Fig. 5. Palladium (Pd), and Pt have almost the same spatial distribution patterns (Fig. 5). These are found to have high spots in the central-eastern parts, Cu has high concentration levels in the southwestern (SW) parts of the area (Fig. 5). Arsenic has high spots in the area except in the SE most and northwestern fringes of the area (Fig. 5). The concentration of As in the area has defined an NE—SW trend in the area. On the contrary, Pb has a concentration trend that is opposite to that of As, with a NW—SE trend. Gold has high values located in the SE in most parts and relatively high levels in the central parts as well.

Gold occurrence can be found within the areas indicating high to moderate concentrations of Pd, Pt, Cu, and As (Fig. 5). However, the spatial distribution of Pb has spots of Au concentration within it, suggesting that Pb cannot be entirely precluded in the search for Au within the area. This corroborates with the approaches applied in the study. Lead is however at the broader location of Au but not locally concentrated in high Au concentration zones within the area.

5 Conclusion

The findings from the study can be summarized as follows;

The trace elements; Cu, Ni, Co, Cr, V, Mg, Fe, Ti as well as Al, correlate well with Au, Pd, Pt, and As. Pb also correlates well with Al, U, Th, Ba, La, and K and correlates negatively with Au. The multivariate statistical approaches thus cluster and factor analysis, indicate similar elemental associations. The pathfinder elements from the study as revealed by all the data analytical approaches; Spearman's correlation matrix, cluster and factor analysis, and MLR, are Pd, Pt, As, and Cu. These are in the order of Pd > Pt > As > Cu. Pb is not a pathfinder element to Au occurrence in the area from the study. The Au in the area is probably controlled by mafic–ultramafic intrusive igneous rocks in the area. The southwestern fringe of the area exhibits high concentrations of Au, Pd, and Pt. Additionally, elevated values of Pd and Pt can also be found at the central, south, and southeastern fringes of the area. Gold has a peculiar local distribution pattern with As. The development of alluvial Au mining in the area is worth exploring.

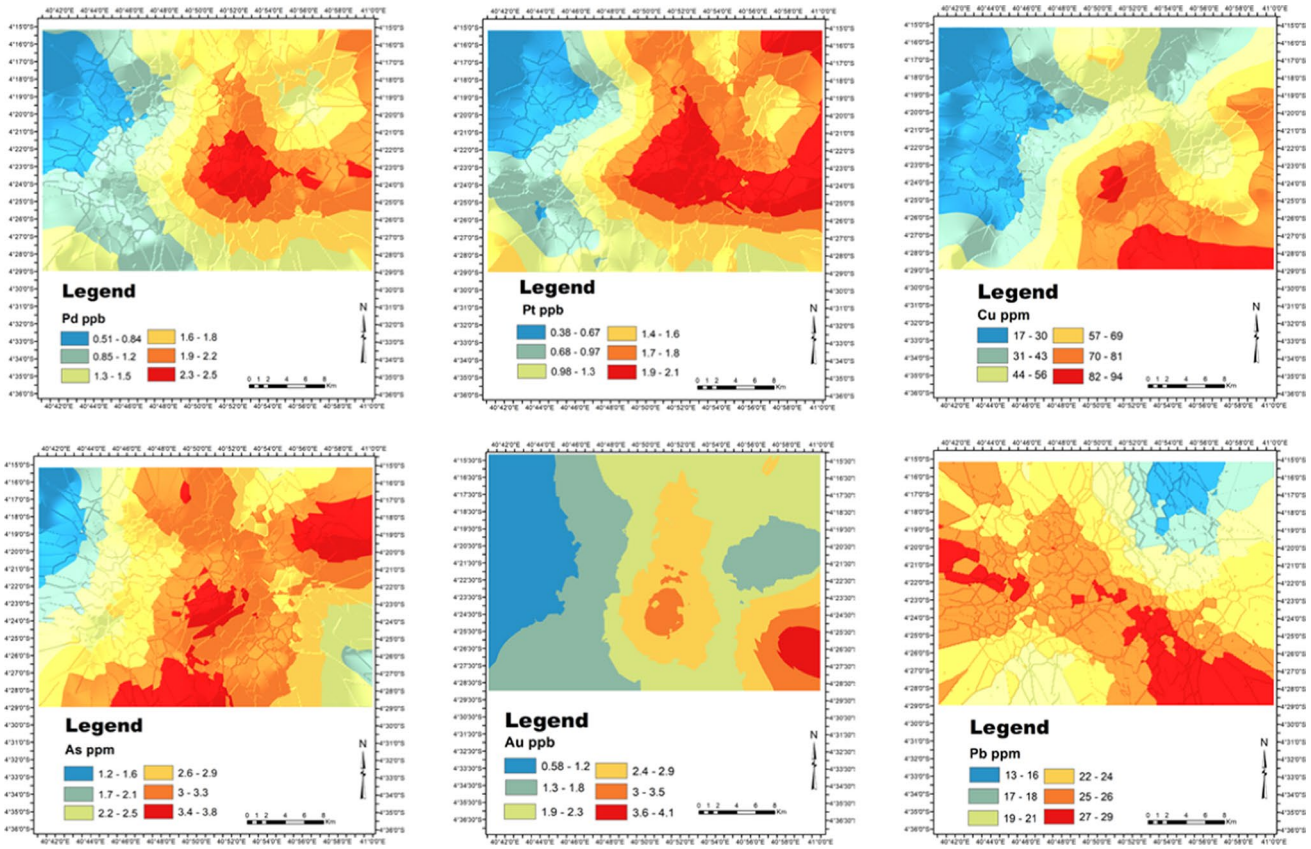

Fig. 5 Spatial distribution of Pd, Pt, Cu, As, Au, and Pb

Acknowledgements The authors are thankful to the Geological Survey of Tanzania (GST) for making available the data needed for the study. Furthermore, they would like to acknowledge Mr. Mjuni Desdery from GST for his valuable contribution in creating the geological map (Fig. 1) used in this work.

Author contributions M.A: Conceptualization, data interpretation, annotation of figures, writing original manuscript draft, text editing, final manuscript review, supervision J.D.K: Field Work, data interpretation, annotation of figures, text editing, final manuscript review B.N.M: Conceptualization, data interpretation, writing original manuscript draft, text editing, final manuscript review, manuscript submission S.N: Data interpretation, text editing, final manuscript review.

Funding No funding.

Data availability The data will be made available on request.

Declarations

Ethics approval and consent to participate Not applicable.

Consent for publication Not applicable.

Competing interests The authors declare no competing interests.

References

1. Hentschel T, Hruschka F, Priester M. Global report on artisanal & small-scale mining. Mining Minerals and Sustainable Development. 2002; 70.
2. Hilson G. Small-scale mining and its socio-economic impact in developing countries. Nat Res Forum. 2002;26:3–13.
3. Ledwaba PF. The status of artisanal and small-scale mining sector in South Africa: tracking progress. J South Afr Inst Min Metall. 2017. https://doi.org/10.17159/2411-9717/2017/v117n1a6.
4. Tanzania Chamber of Mines and Energy. 2015. http://www.tcme.or.tz/miningin-tanzania/industry-overview.
5. Day S, Fletcher K. Particle size and abundance of gold in selected stream sediments, southern British Columbia, Canada. J Geochem Explor. 1986;26(3):203–14.
6. Carranza EJM. Geochemical anomaly and mineral prospectivity mapping in GIS. Handbook of Exploration and Environmental Geochemistry 2009; Vol. 11, M. Hale (Series Editor).
7. Reis AP, Silva EF, Sousa AJ, Patinha C, Martins E, Guimarães C, Nogueira P, et al. Geochemical associations and their spatial patterns of variation in soil data from the Marrancos gold–tungsten deposit: a pilot analysis. Geochemistry. 2009;9(4):319–40.
8. Wang W, Zhao J, Cheng Q. Analysis and integration of geo-information to identify granitic intrusions as exploration targets in southeastern Yunnan District, China. Comp Geosci. 2011;37(12):1946–57.
9. Turnbull R, Martin A, Rattenbury M, Christie A, Sterk R. Regional soil geochemical baseline data for mineral exploration, southern New Zealand. In: Proceedings of the 480th annual conference, New Zealand Branch of the Australasian Institute of Mining and Metallurgy.2015.
10. Mvile BN, Abu M, Kalimenze J. Trace elements geochemistry of in situ regolith materials and their implication on gold mineralization and exploration targeting, Dodoma region, East Africa. Min Metall Explor. 2021;38(5):2075–87.
11. Nunoo S, Mvile BN, Abu M, Kelimenze JD. The search for plausible economic mineral deposits in the central parts of Tanzania; insight from stream sediment geochemistry, multivariate statistics and geostatistics. Heliyon. 2023;9: e22702. https://doi.org/10.1016/j.heliyon.2023.e22702.
12. Kabete JM, Groves DI, McNaughton NJ, Mruma AH. A new tectonic and temporal framework for the Tanzanian Shield: implications for gold metallogeny and undiscovered endowment. Ore Geol Rev. 2012;48:88–124.
13. Salminen R, Kashabano J, Myumbilwa Y, Petro FN, Partanen M. Indications of deposits of gold and platinum group elements from a regional geochemical stream sediment survey in NW Tanzania. Geochemistry. 2008;8(3–4):313–22.
14. Koegelenberg C, Kisters AFM. Tectonic wedging, back-thrusting and basin development in the frontal parts of the Mesoproterozoic Karagwe-Ankole belt in NW Tanzania. J Afr Earth Sc. 2014;97:87–98.
15. Koegelenberg C, Kisters AF, Harris C. Structural controls of fluid flow and gold mineralization in the easternmost parts of the Karagwe-Ankole Belt of north-western Tanzania. Ore Geol Rev. 2016;77:332–49.
16. Sanislav IV, Wormald RJ, Dirks PHGM, Blenkinsop TG, Salamba L, Joseph D. Zircon U-Pb ages and Lu–Hf isotope systematics from late-tectonic granites, Geita Greenstone Belt: implications for crustal growth of the Tanzania Craton. Precambr Res. 2014;242:187–204.
17. Sanislav IV, Dirks PHGM, Cook YA, Blenkinsop TG, Kolling SL. A giant gold system, Geita Greenstone Belt, Tanzania. Acta Geol Sin. 2014;2014(88):110–1.
18. Kalimenze JD, Abu M, Mvile BN. Soil geochemistry and multivariate statistical assessment of Copper-Gold- PGEs mineralization in parts of Singida region of the Tanzania Craton, Tanzania, East African. Arab J Geosci. 2023;16:59. https://doi.org/10.1007/s12517-022-11148-5.
19. Yilmaz H, Sonmez FN, Carranza EJM. Discovery of Au–Ag mineralization by stream sediment and soil geochemical exploration in metamorphic terrain in western Turkey. J Geochem Explor. 2015;158:55–73.
20. Wang W, Wang S, Ma X, Gong J. Recent advances in catalytic hydrogenation of carbon dioxide. Chem Soc Rev. 2011;40(7):3703–27.
21. Sunkari ED, Appiah-Twum M, Lermi A. Spatial distribution and trace element geochemistry of laterites in Kunche area: Implication for gold exploration targets in NW, Ghana. J Afr Earth Sci. 2019;158: 103519.
22. Egbueri JC, Agbasi JC. Combining data-intelligent algorithms for the assessment and predictive modeling of groundwater resources quality in parts of southeastern Nigeria. Environ Sci Pollut Res. 2020;29(38):57147–71. https://doi.org/10.1007/s11356-022-19818-3.
23. Egbueri JC. A multi- model study for understanding the contamination mechanisms, toxicity and health risks of hardness, sulfate, and nitrate in natural water resources. Environ Sci Pollut Res. 2023;30(22):61626–58. https://doi.org/10.1007/s11356-023-26396-5.
24. Kouadri S, Elbeltagi A, Islam ART, Kateb S. Performance of machine learning methods in predicting water quality index based on irregular data set: application on Illizi region (Algerian southeast). Appl Water Sci. 2021;11:190. https://doi.org/10.1007/s13201-021-01528-9.
25. Kontos YN, Kassandros T, Perifanos K, Karampasis M, Katsifarakis KL, Karatzas K. Machine learning for groundwater pollution source identification and monitoring network optimization. Neural Comput Appl. 2022;34:19515–45. https://doi.org/10.1007/s00521-022-07507-8.
26. Gawusu S, Mvile BN, Abu M, Kalimenze JD. Machine learning based prospect targeting: A case of gold occurrence in central parts of Tanzania, East Africa. Ore Energy Resour Geol. 2024;17: 100065.
27. Abu M, Mvile BN, Kalimenze JD. Provenance studies of Au-bearing stream sediments and performance assessment of machine learning-based models: insight from whole-rock geochemistry central Tanzania, East Africa. Environ Earth Sci. 2024. https://doi.org/10.1007/s12665-024-11419-2.
28. Clifford TN. The structural framework of Africa. In African magmatism and tectonics. Oliver and Boyd Edinburgh, 1970; pp. 1–26.
29. Sanislav IV, Brayshaw M, Kolling SL, Dirks PHGM, Cook YA, Blenkinsop TG. The structural history and mineralization controls of the world-class Geita Hill gold deposit, Geita Greenstone Belt, Tanzania. Miner Deposita. 2017;52(2):257–79.
30. Chadha DS. Brief explanation of the geology of Quarter Degree Sheet 162 Dodoma. 1967; (Unpubl. rep.) File 3097.
31. Mshiu EE, Gläßer C, Borg G. Identification of hydrothermal paleofluid pathways, the pathfinders in the exploration of mineral deposits: a case study from the Sukumaland Greenstone Belt, Lake Victoria Gold Field, Tanzania. Adv Space Res. 2015;55(4):1117–33.
32. Mpangile Z, Kazimoto E, Msabi M. Reconnaissance exploration for gold in the Misaki area within the Iramba-Sekenke greenstone belt, central Tanzania, Tanzania. J Sci. 2020;46(1):151–70.
33. Sunkari ED, Abu M, Bayowobie PS, Dokuz UE. Hydrogeochemical appraisal of groundwater quality in the Ga west municipality, Ghana: implication for domestic and irrigation purposes. Groundw Sustain Dev. 2019;8:501–11.

34. Nude PM, Asigri JM, Yidana SM, Arhin E, Foli G, Kutu JM. Identifying pathfinder elements for gold in multi-element soil geochemical data from the Wa-Lawra Belt, Northwest Ghana: a multivariate statistical approach. Int J Geosci. 2012;3(01):62.
35. Sadeghi M, Morris GA, Carranza EJM, Ladenberger A, Andersson M. Rare earth element distribution and mineralization in Sweden: an application of principal component analysis to FOREGS soil geochemistry. J Geochem Explor. 2013;133:160–75.
36. Daviran M, Maghsoudi A, Cohen DR, Ghezelbash R, Yilmaz H. Assessment of various fuzzy c-mean clustering validation indices for mapping mineral prospectivity: combination of multifractal geochemical model and mineralization processes. Nat Resour Res. 2019;29(1):229–46.
37. Daviran M, Maghsoudi A, Ghezelbash R, Pradhan B. A new strategy for spatial predictive mapping of mineral prospectivity: Automated hyperparameter tuning of random forest approach. Comput Geosci. 2021;148: 104688.
38. Koklu R, Sengorur B, Topal B. Water quality assessment using multivariate statistical methods—a case study: Melen River System (Turkey). Water Resour Manage. 2010;24(5):959–78.
39. Wu J, Li P, Wang D, Ren X, Wei M. Statistical and multivariate statistical techniques to trace the sources and affecting factors of groundwater pollution in a rapidly growing city on the Chinese Loess Plateau. Hum Ecolo Risk Assess Int J. 2020. https://doi.org/10.1080/10807039.2019.1594156.
40. Nesbitt H, Young GM. Early Proterozoic climates and plate motions inferred from major element chemistry of lutites. Nature. 1982;299(5885):715–7.
41. Taylor SR, McLennan SM. The continental crust: its composition and evolution. 1985.
42. Dampare SB, Shibata T, Asiedu DK, Osae S, Banoeng-Yakubo B. Geochemistry of Paleoproterozoic metavolcanic rocks from the southern Ashanti volcanic belt, Ghana: petrogenetic and tectonic setting implications. Precambr Res. 2008;162(3–4):403–23.
43. Carranza EJM, Sadeghi M, Billay AY. Data integration for interpretive bedrock mapping in the Giyani area (South Africa). 2013.
44. Sakyi PA, Manu J, Su BX, Kwayisi D, Nude PM, Dampare SB. Geochemical and Sm–Nd isotopic evidence for the composition of the Palaeoproterozoic crust of the West African Craton in Ghana. Geol J. 2018;54(6):3940–57.
45. Abu M, Sunkari ED. Geochemistry and petrography of beach sands along the western coast of Ghana: implications for provenance and tectonic settings. Turk J Earth Sci. 2020;29(2):363–80.
46. Anani CY, Mahamuda A, Kwayisi D, Asiedu DK. Provenance of sandstones from the Neoproterozoic Bombouaka Group of the Volta Basin, northeastern Ghana. Arab J Geosci. 2017;10(21):1–15.
47. Zango MS, Pelig-Ba KB, Anim-Gyampo M, Gibrilla A, Abu M. Assessment of the mineralogy of granitoids and associated granitic gneisses responsible for groundwater fluoride mobilization in the Vea catchment, Upper East Region, Ghana. Sustain Water Resour Manage. 2022;8(1):1–10.
48. Sunkari ED, Seidu J, Ewusi A. Hydrogeochemical evolution and assessment of groundwater quality in the Togo and Dahomeyan aquifers, Greater Accra Region, Ghana. Environ Res. 2022;208: 112679.
49. Angélica RS, da Costa ML, Pöllmann H. Gold, wolframite, tourmaline-bearing lateritized gossans in the Amazon region, Brazil. J Geochem Explor. 1996;57(1–3):201–15.
50. Amponsah PO, Salvi S, Didier B, Baratoux L, Siebenaller L, Jessell M, Gyawu EA. Multistage gold mineralization in the Wa-Lawra greenstone belt, NW Ghana: the Bepkong deposit. J Afr Earth Sc. 2016;120:220–37.
51. Basu S, Lokesh KS. Application of multiple linear regression and manova to evaluate health impacts due to changing river water quality. Appl Math. 2014. https://doi.org/10.4236/am.2014.55076.
52. Daviran M, Ghezelbash R, Maghsoudi A. GWOKM: a novel hybrid optimization algorithm for geochemical anomaly detection based on Grey wolf optimizer and K-means clustering. Geochemistry. 2024;84: 126036. https://doi.org/10.1016/j.chemer.2023.126036.
53. Ghezelbash R, Daviran M, Maghsoudi A, Ghaeminejad H, Niknezhad M. Incorporating the genetic and firefly optimization algorithms into K-means clustering method for detection of porphyry and skarn Cu-related geochemical footprints in Baft district, Kerman, Iran. Appl Geochem. 2023;148: 105538. https://doi.org/10.1016/j.apgeochem.2022.105538.
54. Nunoo S, Abu M, Ayitey E, Mvile BN, Kalimenze JD. Multi-method machine learning techniques in gold pathfinder elements prediction in central parts of Tanzania using stream sediment geochemical data. Phys Chem Earth. 2024;136: 103766. https://doi.org/10.1016/j.pce.2024.103766.